TES Bolometer and DfMux Readout Characterization for POLARBEAR-2B

Tucker Elleflot
University of California San Diego
Department of Physics
tuckerelleflot@gmail.com

and K. Arnold, D. Barron, K. T. Crowley, M. Dobbs, J. Groh, M. Hasegawa, M. Hazumi, C. Hill, L. Howe, J. Ito, O. Jeong, D. Kaneko, B. Keating, A. Kusaka, A. T. Lee, L. N. Lowry, C. Raum, J. Seibert, M. Silva-Feaver, P. Siritanasak, A. Suzuki, S. Takakura, S. Takatori, C. Tsai, B. Westbrook

Abstract

POLARBEAR-2B (PB-2B) is the second of three cryogenic receivers of the Simons Array (SA) Cosmic Microwave Background (CMB) polarization experiment. SA will measure mid- to large-scale CMB anisotropies in order to constrain the tensor-to-scalar ratio ($\sigma(r = 0.1) = 6 \times 10^{-3}$) and the sum of the neutrino masses ($\sigma(\sum m_\nu = 40\,meV)$). PB-2B contains over 7,500 Transition Edge Sensor (TES) bolometers cooled to 250 mK and read out using Digital Frequency-Division Multiplexing (DfMux). Stray impedance in the DfMux circuit impacts TES characterization and TES performance. Here we report in-lab characterization of the DfMux circuit and TES wafers that will be fielded with PB-2B.

1 Digital Frequency-Division Multiplexing (DfMux)

POLARBEAR-2B uses DfMux [1] to simultaneously bias and measure 40 detector channels with a single pair of wires between the 4 K SQUID amplifier and the 250 mK detector stage. Each detector is put in series with a resonant LC filter with a unique resonance frequency. An AC voltage bias is created by driving a current, $I_{carrier}$, through a $30\,m\Omega$ bias resistor, R_{bias}, and applied to the entire set of detectors. In the analysis below, we will consider a simplified model of the bias circuit as seen by an individual TES in which we combine the multiple sources of stray impedance into a stray series impedance and stray bias inductance.

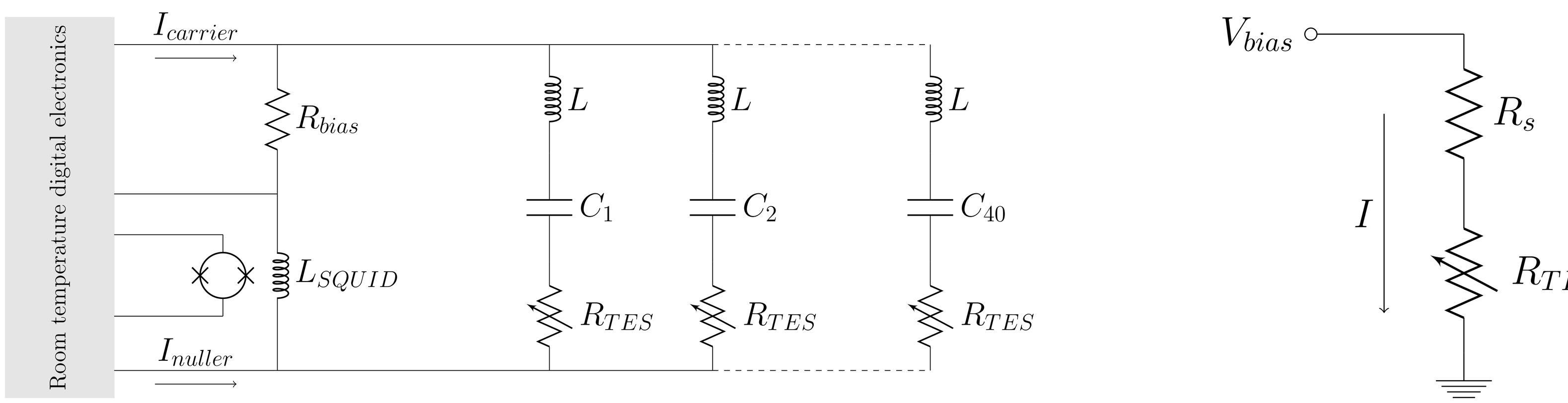

Figure 1: Left: DfMux circuit used to bias and measure TES detectors in PB-2B receiver. Right: Bias circuit seen by a single detector in DfMux scheme. R_s is a stray series resistance that arises from stray inductance in cryogenic wiring and connectors, dielectric loss in capacitors, and contact resistance of connectors.

1.1 Stray Series Resistance

Stray series resistance in the DfMux circuit forms a voltage divider with each TES (Fig. 1). The voltage bias and voltage across the TES, respectively, are given by:

$$V_{bias} = I_{carrier} R_{bias} \quad (1)$$

and

$$V_{TES} = V_{bias}\frac{R_{TES}}{R_{TES}+R_s}. \quad (2)$$

We measure R_s (R_n) by taking the ratio of V_{bias} (V_{TES}) to I when the TES is superconducting (normal).

1.2 Stray Bias Inductance

Figure 2 shows that R_n as measured using the technique in Sec. 1.1 has a residual dependence on bias frequency. This is explained by a stray bias inductance in series with R_{bias} in Fig. 1, which causes us to underestimate V_{bias} at high bias frequencies [2]. Because resistance and power are calculated using V_{bias}, they are underestimated as well. The impedance of the stray bias inductance is $6\,m\Omega(\frac{f_{bias}}{1\,MHz})(\frac{L_{bias}}{1\,nH})$.
To measure the stray bias inductance, we assume that the TES normal resistances do not depend on bias frequecy and that the trend we see is due to a stray bias inductance. We simultaneously fit the normal resistance measurements for an entire TES wafer using a model with one stray bias inductance per bias resistor and one TES normal resistance.
Once we have determined the stray bias inductance values, we apply the below multiplicative correction to all measured voltages, resistances, and powers

$$\left|\frac{R_{bias}+i\omega L_{bias}}{R_{bias}}\right|. \quad (3)$$

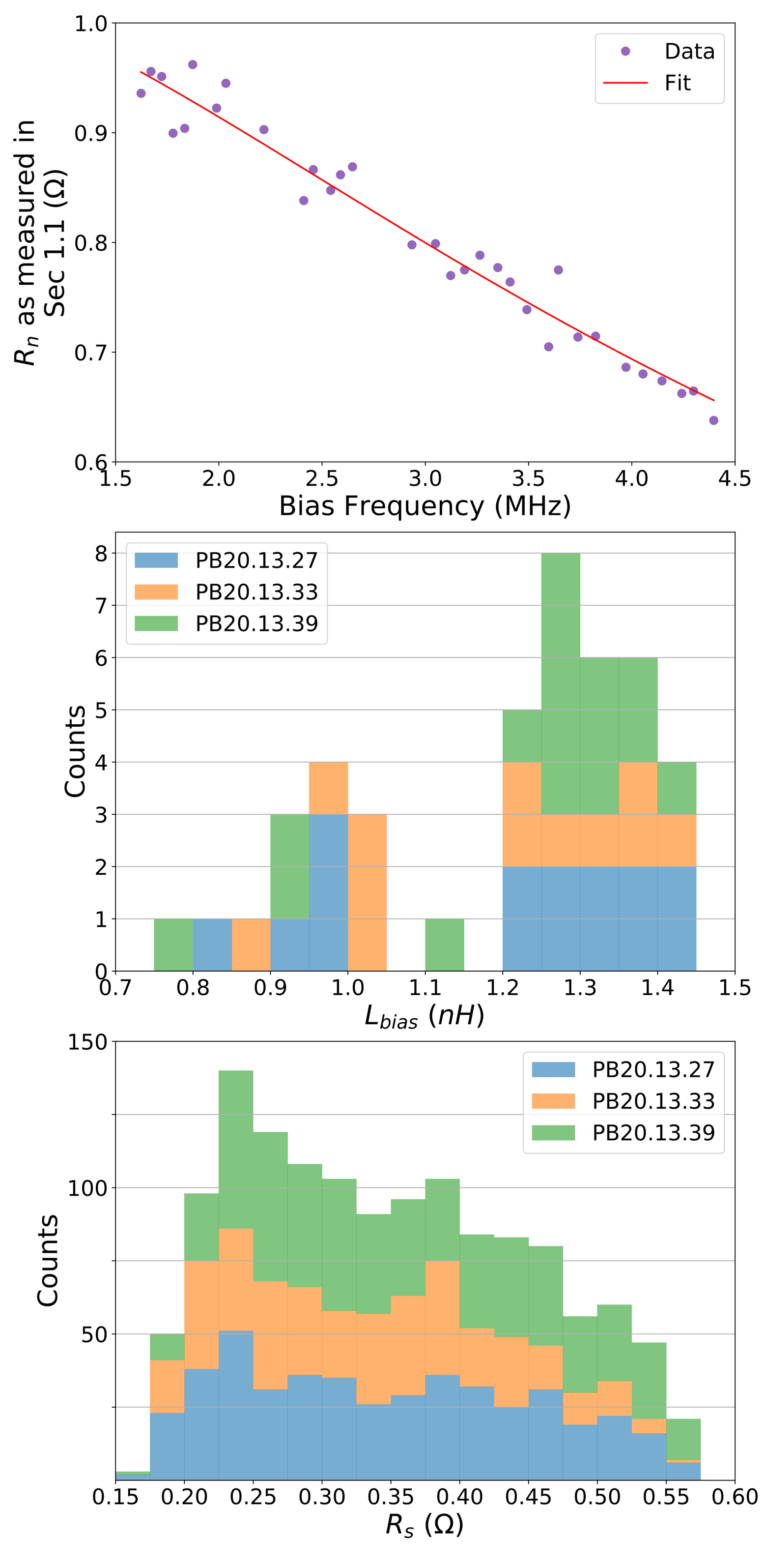

Figure 2: Top: R_n measured as described in Sec. 2.1 and best-fit model from Sec. 2.2 are plotted against bias frequency. Middle: A histogram of L_{bias} values for forty-three bias resistors measured as described in Sec. 2.2 is shown. Bottom: Series stray resistance values measured for over 1,300 TESs on three TES wafers are shown. The stray bias inductance correction described in Sec. 1.2 has been applied.

2 TES Characterization

2.1 TES Power Balance with Stray Series Impedance

Following [3], we derive the small-signal power balance equation. Conservation of energy requires:

$$\delta P_{opt} + \delta P_{elec} + \delta P_{bath} = i\omega\delta E. \quad (4)$$

To simplify notation, we will drop the subscript on V_{bias} and refer to it as V and a subscript 0 will represent a steady-state value. The quantities of most interest to us are δV, δI, and δP_{opt} since they are what we can control and/or want to measure. Using a first-order Taylor series expansion of Ohm's law and $R = R(T)$, we can express Eq. 4 as

$$\frac{\delta P_{opt}}{P_{elec,0}} = -\frac{1}{\mathcal{L}}\left(\frac{R_{TES,0}+R_s}{R_{TES,0}}\right)\left[\left(\mathcal{L}-1-i\omega\tau_0\right)\frac{\delta V}{V_0}+\left(\mathcal{L}\left(\frac{R_{TES,0}-R_s}{R_{TES,0}+R_s}\right)+1+i\omega\tau_0\right)\frac{\delta I}{I}\right]. \quad (5)$$

In Eq. 5, $\mathcal{L}$ is the TES loop gain defined as $\mathcal{L} \equiv \frac{\alpha P_{elec}}{GT}$ and τ_0 is the intrinsic time constant of the TES.

2.2 IV Curves

We measure IV curves to characterize PB-2B TESs as described in [4] with the addition of the stray bias inductance correction as described in Section 1.2. Additionally, we use equation 4 to calculate loop gain from IV curves. Considering that the voltage steps are done slowly and under constant optical loading, the loop gain is given by the below equation:

$$\mathcal{L} = \frac{1-(R_{TES,0}+R_s)\frac{\delta I}{\delta V}}{1+(R_{TES,0}-R_s)\frac{\delta I}{\delta V}} \quad (6)$$

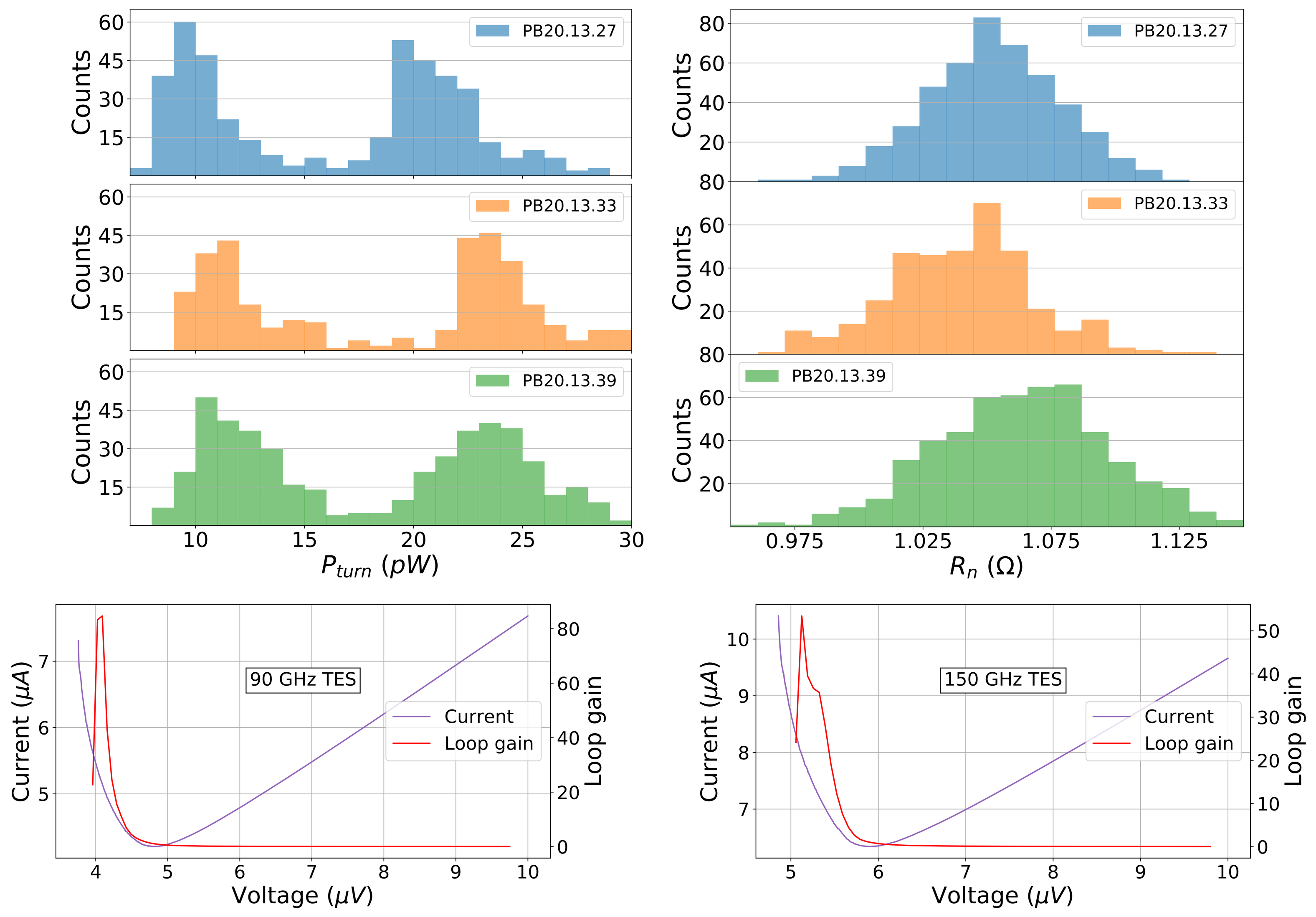

Figure 3: Top left and right: Histograms of turnaround power and normal resistance, respectively, for three TES wafers that will deploy with PB-2B. The turnaround powers are bimodal because PB-2B will observe in two frequency bands. The lower power band is for 90 GHz observations and the higher power band is for 150 GHz observations. Bottom left and right: Current and loop gain plotted as a function of applied voltage bias for detectors optimized for 90 and 150 GHz.

2.3 Responsivity and Time Constant

The TES responsivity and time constant under a constant voltage bias can be derived from equation 5:

$$S_I \equiv \frac{\delta I}{\delta P_{opt}} = -\frac{1}{V_0}\frac{\mathcal{L}}{\mathcal{L}\frac{R_{TES,0}-R_s}{R_{TES,0}+R_s}+1+i\omega\tau_0} \quad (7)$$

$$\tau = \frac{\tau_0}{\mathcal{L}\frac{R_{TES,0}-R_s}{R_{TES,0}+R_s}+1} \quad (8)$$

Equation 8 shows that the time constant is increased by the presence of a series parasitic impedance. This is because the series impedance weakens the voltage bias on the TES and reduces the effectiveness of electrothermal feedback.
We measured the time constants of tuned detectors using a thermal source chopped at frequencies between 4 Hz and 33 Hz. At each tuning point, the chop frequency was varied and the TES response was fit to a single-pole model to retrieve τ. We fit the model in equation 8 to the measured loop gain, resistance, and time constant data to obtain a value of τ_0.

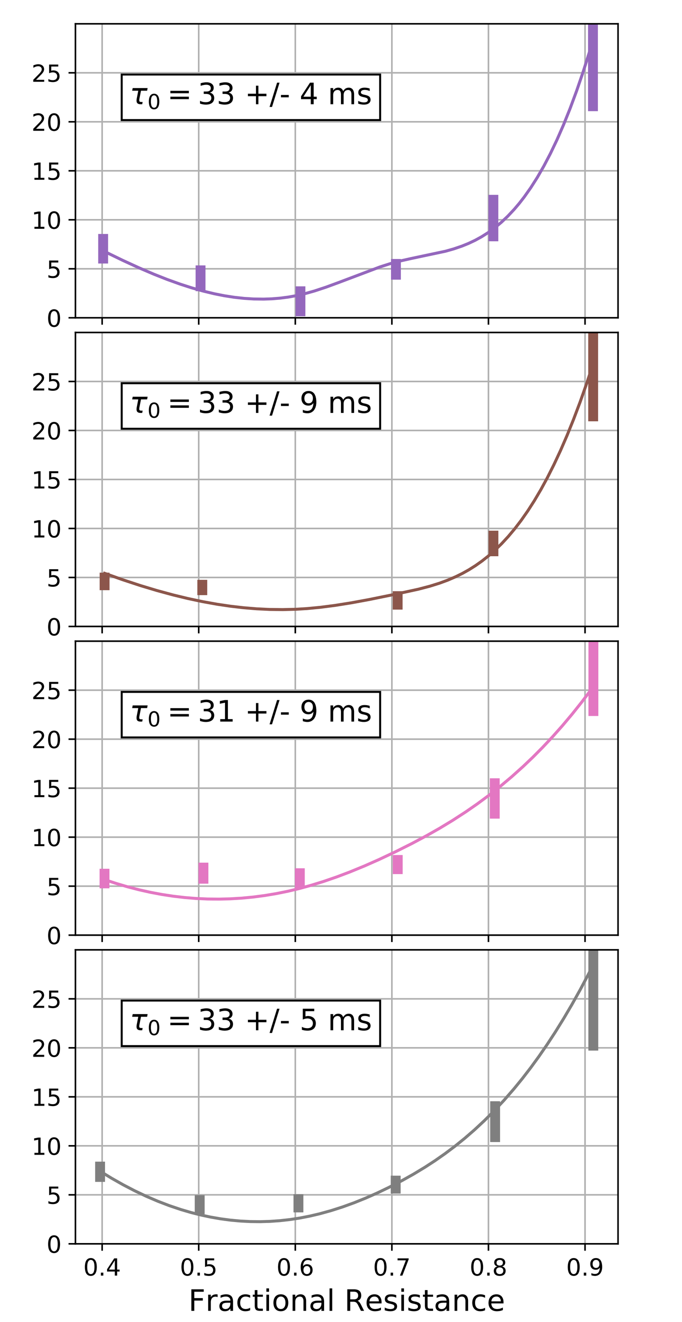

Figure 4: Measured time constant plotted against fractional TES resistance for four TES detectors. Fractional resistance is defined here as $\frac{R_{TES}+R_s}{R_n+R_s}$. The data are fit to the model in equation 8 and the fitted time constant is shown for each.

References

1. M. Dobbs et al., Frequency multiplexed superconducting quantum interference device readout of large bolometer arrays for cosmic microwave background measurements. Rev. Sci. Instrum. 83, 073113 (2012).
2. J. Montgomery, Masters Thesis. Development of Multiplexed Bolometer Readout Electronics for mm-wave Space Astronomy. McGill University 2015.
3. K. D. Irwin and G. C. Hilton, "Transition-edge sensors," in Cryogenic Particle Detection, edited by C. Enss (Springer-Verlag, 2005), Vol. 99, pp. 63–149.
4. T. Elleflot, Y. Akiba, K. Arnold, et al., Detector and Readout Assembly and Characterization for the Simons Array, Journal of Low Temperature Physics, Special Issue "Low Temperature Detectors LTD-17".

Acknowledgements

The Simons Array is supported by the Simons Foundation, the National Science Foundation (AST-1440338), the Moore Foundation, and the Heising-Simons Foundation.